Study of photoinduced magnetism in crystals on a SQUID magnetometer

G. S. Patrin, D. A. Velikanov, and I. A. Petrakovskiĭ

L. V. Kirenskiĭ Institute of Physics, Siberian Branch of the Russian Academy of Sciences
(Submitted 24 June 1992)
Zh. Eksp. Teor. Fiz. **103**, 234–251 (January 1993)

We present the results of an experimental and theoretical investigation of photoinduced change in the magnetic moment in $FeBO_3$ crystals. A SQUID magnetometer, equipped with an optical pumping system, was employed in the experiment. By studying the field, temperature, and time dependences of the photoinduced change in the magnetic moment at various optical powers we were able to determine the mechanism responsible for the change in the magnetic state under irradiation. All experimental results are explained within a model where the crystal matrix is described in the continuous approximation and the photocenter (supposedly and Fe^{2+} ion) is described as a quasi-Ising ion with $\tilde{S} = 1$, exchange-coupled to one of the magnetic sublattices of the crystal. Under irradiation the populations of the levels in the ground-state multiplet are redistributed in a manner such that, because of the selection rules for optical transitions, the more anisotropic level is predominantly populated. The model employed made it possible to calculate and explain the anisotropic properties of $FeBO_3$ crystals and the spin-reorientation transition in the basal plane at low temperatures.

INTRODUCTION

There are many reasons for the current interest in $FeBO_3$ crystals. On the one hand, these crystals already have practical applications in millimeter-range microwave devices.[1] On the other hand, they also have a rich set of physical properties and they serve as model crystals for studying many pheonmena. One of the interesting properties of $FeBO_3$ crystals is their photosensitivity, first observed as a change in the magnetic susceptibility under irradiation with white light.[2] Later the effect of light on the magnetoacoustic resonance[3] and optical linear birefringence[4] were investigated, and induction of long-period magnetic structure[5] was observed. However, all of these experiments were performed at liquid-nitrogen temperatures, which is a limiting factor in establishing the mechanisms responsible for the photosensitivity of $FeBO_3$ crystals.

The first investigations of the photomagnetic effect at liquid-helium temperatures were performed on $FeBO_3$:Ni crystals by the antiferromagnetic resonance (AFMR) method.[6] It was then observed that the time variation of the photoinduced shift of the resonance field in time can be divided arbitrarily into two stages: fast changes (reversible, timed in seconds) and slow changes (irreversible, timed in minutes). In the investigation of irreversible photoinduced changes in crystals, both containing different impurities and nominally pure, it has been found[7,8] that irradiation changes the AFMR linewidths and the temperature behavior of the resonance field. In addition, the low-temperature maximum, attributed to the presence of bivalent iron ions in $FeBO_3$ crystals, decreases in magnitude against the background of a general increase in the value of the resonance field. These magnetoresonance experiments were interpreted as redistribution of Fe^{2+} ions by means of charge transfer between nonequivalent crystallographic positions in the process of light absorption.

We present below the results of a study of the temporal behavior of the reversible light induced change in the component of the magnetic moment in the direction of the external magnetic field by the SQUID magnetometry method.

EXPERIMENT

The measurements were performed on nominally pure bulk $FeBO_3$ single crystals with an average transverse size of 1.5 mm. The crystals were grown by the method of spontaneous crystallization from a molten solution. The light propagated in the direction of the external magnetic field. The latter field was perpendicular to the C_2 axis and lay in the basal plane of the crystal. The crystal was oriented with respect to the direction of the magnetic field with an accuracy of $\pm 5°$. The light source was a helium-neon laser with $\lambda = 0.63\ \mu$m.

A SQUID magnetometer was chosen as the instrument for the investigation. This magnetometer has an extremely high sensitivity ($10^{-4}\ \mu V/\Phi_0$, where Φ_0 is the magnetic flux quantum), which makes it possible to perform delicate measurements in weak magnetic fields. The sensitivity of this method, in contrast to force methods for measuring the magnetic susceptibility, does not depend on the average intensity of the signal against whose background the induced changes are measured.

The measurements were performed on a SQUID magnetometer described in Ref. 9. We employed a cryogenic attachment with a lightguide, as shown in Fig. 1. The laser light was directed through a system of lenses into the end of the lightguide, which was at room temperature. The distance between the surface of the sample and the cold end of the lightguide was 0.5 mm. The sample was located at the bottom of an ampul in a stress-free state. The power of the laser radiation incident on the sample was calibrated with an optical power meter. For this, the cold end of the lightguide was placed in the measuring head, and the conditions of the experiment were reproduced as closely as possible.

An Fe/Au-Cu thermocouple, whose cold junction was

 1063-7761/93/010128-10$10.00

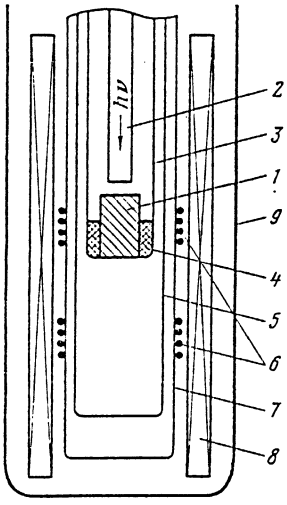

FIG. 1. Schematic of the cryogenic insert with the sample: *1*—sample, *2*—lightguide, *3*—ampul, *4*—insert, *5*—attachment, *6*—detecting coils of a superconducting magnetic-flux transformer, *7*—framework, *8*—superconducting solenoid, *9*—magnetic screen.

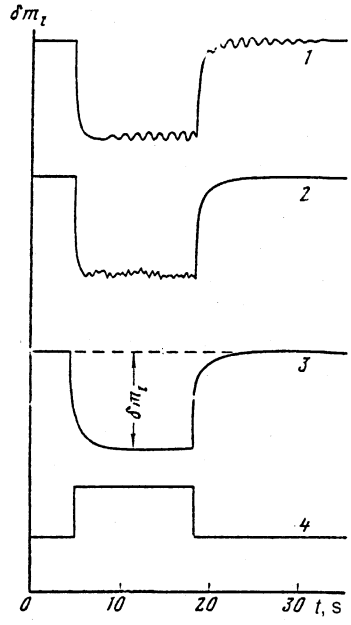

FIG. 2. Time dependence of the photoinduced change in the magnetic moment at $T = 2$ K (*1*), 6 K (*2*), and 16 K (*3*); *4*—light pulse.

located 3 mm above the sample, was used to measure the temperature.

EXPERIMENTAL RESULTS

In the experiment we measured the change in the projection of the magnetic moment on the direction of the external magnetic field upon illumination. Figure 2 shows the light pulse (curve 4) and the photoinduced changes in the magnetic moment of the sample (curves 1–3). The width of the light pulse was chosen so that there would be enough time for the measured quantity to reach a stationary value. We next tracked the maximum change in the magnetic moment, denoted as δm_l. Under prolonged irradiation, after the light is switched off the change in the magnetic moment does not return to the initial zero marker, but rather a small residual moment, which remains constant in time, is observed.

The magnetic field dependences of the photoinduced change in the magnetic moment at different temperatures are presented in Fig. 3, and the changes at different optical pump power levels are presented in Fig. 4. Curve 1 in Fig. 3 and curve 3 in Figure 4 were obtained on the same sample, but in a different series of measurements. For this reason, we attribute the observed difference in these curves to the uncertainty in the placement of the crystal with respect to the external magnetic field. We note that in fields exceeding 300 Oe these curves are identical and behave as shown in Fig. 3. The positive component of the photoinduced change in the magnetic moment is specific to each sample and occurs in virtually all crystals which we studied. It is probably formed by the contribution of the Bloch walls separating domains in the horizontal direction (parallel to the (111) plane) in bulk $FeBO_3$ crystals. We call attention to the fact that at low temperatures the photoinduced component of the magnetic moment decreases with increasing temperature, while the reverse behavior is observed with increasing optical power.

It is obvious (see Fig. 5) from the temperature dependence of δm_l, measured in magnetic fields corresponding to the maximum "negative" and "positive" photoinduced changes in Fig. 3, that at temperatures $T > 30$ K these changes are virtually identical. It is also clear from Fig. 5 that all of these changes occur against the background of a monotonic and smooth decrease (with increasing temperature) of the magnetic moment of the crystal (curve 3) and they are not related with the thermal effect of the optical radiation.

Analysis of the time dependence of the photoinduced change in the magnetic moment showed that the part of the curve corresponding to the descending section is not described by a simple exponential. Its shape at a fixed temperature in the range $T < 50$ K can be described by the formula

$$|\delta m_l(t)| = B_1 \exp(-t/\tau_1) + B_2 \exp(-t/\tau_2). \quad (1)$$

As the temperature increases the "slow" exponential begins to predominate. The parameter τ_1 of the "fast" exponential in the temperature range considered can be approximated by the expression

$$1/\tau_1 = \omega_1 \exp(-\Delta_1/k_B T), \quad (2)$$

where k_B is Boltzmann's constant, $\omega_1 = 1.5\ \text{sec}^{-1}$, and $\Delta_1/k_B = -5.6$ K. The amplitude B_1 decreases by more than an order of magnitude as the temperature changes from 4.2 to 50 K. With regard to the "slow" exponential, we note that the time τ_2 in this temperature range decreases approximately by a factor of two, but its temperature dependence is no longer described by a formula of the type (2). In addition, for agreement with experiment, the quantities ω_2 and Δ_2 must be temperature dependent. Within the framework of an approach in which the impurity system is represented as an ensemble of two-level centers, this behavior can be explained by the existence of centers with a collection of splittings which are close in magnitude. It was established that the thermal contribution, whose relative weight increases with increasing temperature, becomes appreciable at temperatures $T \geqslant 50$ K.

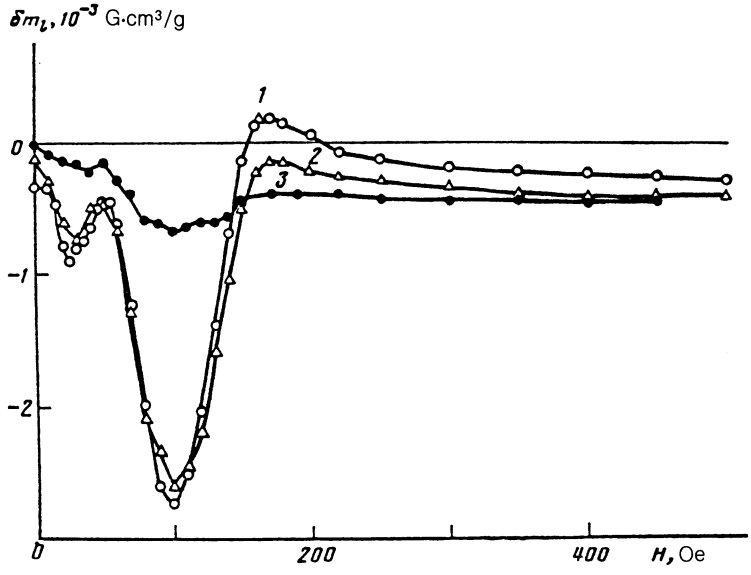

FIG. 3. Field dependences of the photoinduced change in the magnetic moment (experiment) at $T = 4.2$ K (*1*), 6 K (*2*), and 16 K (*3*); $P = 0.1$ W/cm^2.

We discovered a characteristic feature of the time dependence of the photoinduced change in the magnetic moment: an onset of oscillations. According to Fig. 2 (curve 1), when the optical radiation is switched on at $T = 2$ K, self-excited oscillations start to buildup after several seconds. This process becomes stationary and has the form of steady harmonic oscillations. After the light is switched off, the oscillations decay over a time of the order of 10 sec. As the temperature increases up to $T = 6$ K the amplitude of the self-excited oscillations decreases significantly and is virtually indistinguishable from the background noise (Fig. 2, curve 2). The process occurs in magnetic fields 15–70 Oe; no self-excited oscillations were observed in stronger fields. One can also see from Fig. 2 that the time at which the photoinduced component of the magnetic moment saturates increases with increasing temperature.

MODELS

It has now been established reliably that the photosensitivity of $FeBO_3$ crystals is determined by internal factors, which are characteristic of the given sample, and it is not introduced by the dopants. In a number of cases the dopants intensify the sensitivity to irradiation,[2] and as our previous experiments show,[7,8] the technological conditions of the synthesis play a large role. For nominally pure samples it has been established that the wider the AFMR line (i.e., the lower the sample quality) the higher the photosensitivity. It is obvious that in such a case the photosensitivity of the crys-

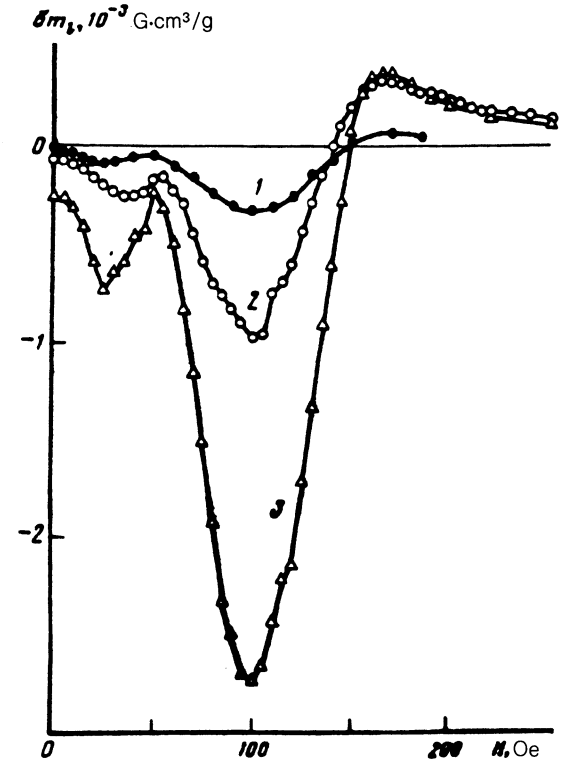

FIG. 4. Field dependences of the photoinduced change in the magnetic moment for optical pump powers (experiment) $P = 0.02$ W/cm^2 (*1*), 0.04 W/cm^2 (*2*), and 0.1 W/cm^2 (*3*). $T = 4.2$ K.

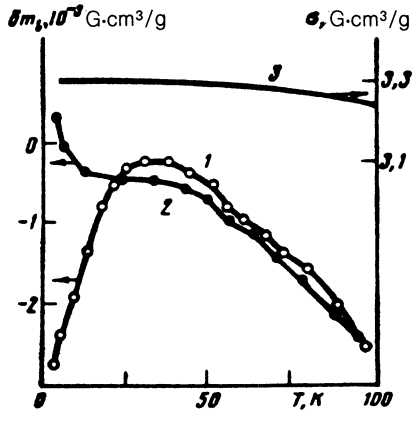

FIG. 5. Temperature dependences of the photoinduced change in the magnetic moment (experiment) in fields $H = 100$ Oe (*1*) and 175 Oe (*2*); *3*—$FeBO_3$ magnetization; $P = 0.1$ W/cm^2.

tal must be related with the existence of iron–oxygen complexes arising at the crystal growth stage and containing bivalent iron ions.

It is known[10] that Fe^{2+} ions in the structure of corundum, which is isomorphic to $FeBO_3$ crystals, can occupy positions held by Al^{3+} ions without any distortion of the crystal. The principal magnetic properties of Fe^{2+} ions in the corundum structure at low temperatures are described by a spin Hamiltonian which includes the Zeeman energy with an anisotropic g factor and uniaxial single-ion magnetic anisotropy for effective spin $\tilde{S} = 1$ with the C_3 axis being the local quantization axis. Crystal-field theory gives $g_\perp = 0$,[11] while the Jahn-Teller analysis gives $g_\perp = 3.3$–5.3;[10] in both cases $g_\parallel = 3.4$, indicating that the orbital angular momentum plays a large role in the formation of the magnetic state of the Fe^{2+} ion. The single-ion anisotropy constant D has the value 4.2 cm^{-1}.

Magnetically,[12] the crystal $FeBO_3$ is a two-sublattice weak ferromagnet of the easy-plane type with $T_N = 348$ K. The strongest interaction is the antiferromagnetic intersublattice exchange interaction; the intrasublattice ferromagnetic interaction is an order of magnitude weaker. An important feature of this crystal is that it undergoes a spin-reorientational phase transition at $T_S = 5$ K, where the direction of easy magnetization changes from the σ symmetry plane to the C_2 axis as the temperature increases, though for different crystals a spread in the values of T_S is observed.[7] Anomalies are observed in the AFMR parameters near this temperature, while no peculiarities are observed in the temperature dependence of the magnetization.

According to Mössbauer spectroscopy data,[13] the temperature dependence of the linewidth (which exhibits weak traces of a fine structure) contains a break at $T = 551$ K. The authors attributed this break to restructuring of the energy spectrum due to a Jahn-Teller transition. For pure $FeBO_3$ the Fe^{3+} ions do not have levels in this region.

We note that calculations for Fe^{2+} in Al_2O_3, taking into account the Jahn-Teller effect, show that an energy level is present near 500 cm^{-1}.[10]

It is well known[14] that boron-containing compounds do not crystallize very well and tend to form a glass with a three-dimensional framework; in addition, boron–oxygen complexes, where the boron ions can be in a B^{4+} state, can form in such compounds. Applied to the case of $FeBO_3$, the presence of such a complex could serve as a catalyst for the appearance of Fe^{2+} ions. In the magnetic respect, the crystals containing bivalent iron ions have sharply anisotropic magnetic properties. For example, for $FeCO_3$ crystals (here the carbon is in the C^{4+} states), which are structurally isomorphic to $FeBO_3$ crystals, the Fe^{2+} ions behave as Ising ions and the entire crystal exhibits metamagnetic properties.[15]

Thus, if it is assumed that the photosensitive center is a complex containing an Fe^{2+} ion, analysis of the results should provide an explanation of all properties characteristic of the crystal in both the ground state and in the presence of different perturbations.

Since for Fe^{2+} the quasidoublet with splitting of about 5 cm^{-1} (Ref. 11), which is observed at low temperatures, has the lowest energy and the next level is quite high, it is most likely that optical irradiation induces redistribution of populations of this quasidoublet. For a two-level system the temperature dependence of the relaxation time to thermodynamic equilibrium will be determined by an expression of the type (3) in the case if irradiation produces in the level with the higher energy an excess population. For this reason, some part of the photoinduced change in the magnetization can be associated with such a mechanism. The relaxational behavior of the other part can be explained within a two-level model assuming that under irradiation the lower energy level acquires excess population. Thus we are forced to consider several nonequivalent centers which react differently to optical irradiation.

Let the impurity ions occupy sites which are characteristic of Fe^{3+} ions, are tied to sites of oxygen vacancies, they are distributed with equal probability over 24 nonequivalent positions in the crystal, differing by the sets of indices $\{k = 1, 2; s = 1, 2; t = 1, ..., 6\} = \{p\}$, indicating respectively, the following: whether the site belongs to the first or the second sublattice; the angle $\pm\alpha$, by which the ξ and η axes of a local coordinate system are turned in the basal plane relative to the crystallographic C_2 axes (the crystal axis X or Y); and, the number of the nonequivalent site in the chosen sublattice. Then we label by the index q the ion located at a selected nonequivalent position. Further, we assume that the quantization axes Z' for Fe^{2+} ions in the local coordinate system coincide with the ξ axes.

All of the conditions stated above can be satisfied simultaneously for an impurity ion located at the (pq)-th position by using a spin Hamiltonian of the form

$$\hat{\mathcal{H}}_{pq} = (-g\mathbf{H}_0 + \lambda\mathbf{M})\beta\tilde{\mathbf{S}}_{Z'_{pq}} + D(S^2_{Z'_{pq}} - {}^2/_3) + E(\tilde{S}^2_{X'_{pq}} - \tilde{S}^2_{Y'_{pq}}), \quad (3)$$

where $\tilde{S}_{pq} = 1$ is the effective spin of an ion, β is the Bohr magniton, λM is the molecular field generated by the other sublattice and acting on the (pq)-th ion, $\mathbf{H}_0$ is the external magnetic field, and D and E are the parameters of the crystal field. For all ions we have $N_k = N_0/2$, $N_{ks} = N_0/4$, $N_{kst} = N_0/24$, and $\Sigma_{\{kstq\}} N_{kstq} = N_0$ is the total number of impurity centers.

Diagonalizing the expression (3) gives the following eigenvalues:

$$\begin{aligned} \varepsilon_{pq}{}^1 &= -2D/3, \\ \varepsilon_{pq}{}^2 &= D/3 - \{[(\lambda M\gamma_{pq} - gH_0\gamma_{pq}')\beta]^2 + E^2\}^{1/2}, \\ \varepsilon_{pq}{}^3 &= D/3 + \{[(\lambda M\gamma_{pq} - gH_0\gamma_{pq}')\beta]^2 + E^2\}^{1/2}, \end{aligned} \quad (4)$$

where γ_{pq} and γ'_{pq} are the cosines of the angles between the corresponding fields acting on the moment of the (pq)-th ion and the local quantization axis Z'.

Figure 6 displays a diagram of the energy levels of the centers as a function of the angle between the direction of magnetization of the sublattice and the local axis Z' for different positions. (Since $|\lambda M| \gg |gH_0|$, the direct contribution from the interaction between the magnetic field and the spin of the ion is neglected.)

If the interference effects between different states are neglected, the behavior of the ensemble of impurity ions in the optical radiation field can be described by the system of kinetic equations

$$\frac{dn_{pq}{}^l}{dt} = \sum_{l \neq m} d_{pq}{}^{lm} n_{pq}{}^m, \qquad l, m = \{1, 2, 3, \psi\}, \quad (5)$$

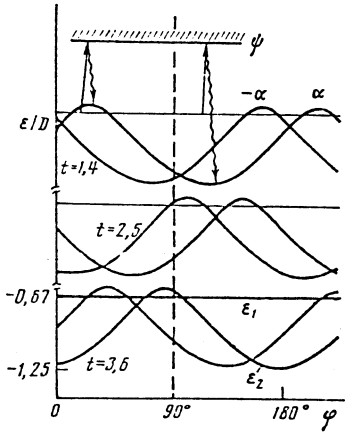

FIG. 6. Diagram of energy levels of impurity centers in different crystallographic positions as a function of the angle between the chosen axis C_2 and an external magnetic field. The arrows indicate the predominant photoinduced transition in a cycle of optical absorption and relaxation.

where ψ is the index of the optically excited state.

For the entire crystal, the condition

$$\sum_{(p,q,l)} n_{pq}{}^{l}=4N_0 \tag{6}$$

is satisfied. Here n_{pq}^{l} is the population of the l-th state and d_{pq}^{lm} is the probability of a transition between the l-th and the m-th levels.

As applied to our case, we assume that optical transitions occur only between the ground states of the center and the optically excited state $|\psi\rangle$, i.e., $|l\rangle \rightarrow |\psi\rangle (l=1,2)$, and that the transition probabilities are functions of the frequency ν and intensity I of the radiation and the temperature T: $d^{l\psi}=d^{l\psi}(\nu,I,T)$. We assume that the transitions $|\psi\rangle \rightarrow |l\rangle$ are nonradiative. Since the optical radiation does not directly induce transitions between levels of the ground-state multiplet of the impurity center, the relaxational transitions between them must satisfy the following condition—because of the detailed-balancing condition, for example for the states $|1\rangle$ and $|2\rangle$:

$$d_{pq}{}^{12}/d_{pq}{}^{21}=\exp(-\Delta_{pq}/k_BT), \quad \Delta_{pq}=\varepsilon_{pq}{}^{2}-\varepsilon_{pq}{}^{1}. \tag{7}$$

On the basis of what was said above, the formulas for the populations of the levels of the center have in the stationary case the form

$$n_{pq}{}^{1}=(1+A_1)/Q, \tag{8a}$$

$$n_{pq}{}^{2}=[\exp(-\Delta_{pq}/k_BT)+A_2]/Q, \tag{8b}$$

and the expressions for A_1, A_2, and Q in terms of the transition probabilities are presented in Ref. 16. Since the energy of the level 3 is quite high and this level does not contribute to the magnetic properties and it also has a very short lifetime [$\tau_{31}\sim 10^{-10}$ sec (Ref. 11)], we can ignore it.

Summing the results (4) and (8), the expression for the energy of the impurity subsystem in the optical radiation field can be written in the form

$$f=\sum_{(p,q,l)} n_{pq}^{l}\varepsilon_{pq}{}^{l}-ST, \tag{9}$$

where S is the entropy of the impurity subsystem.

CALCULATION OF PHOTOINDUCED CHANGES OF THE MAGNETIC PROPERTIES

According to Ref. 17, the magnetic energy of an $FeBO_3$ crystal, taking into account the energy of the impurity subsystem, has the form

$$W=W_Z+W_E+W_D+W_{A0}+f. \tag{10}$$

Since we shall be concerned below only with the situation when the external magnetic field and the magnetic moments of the sublattices lie in the basal plane, the uniaxial anisotropy energy W_{A0} can be dropped. In a spherical coordinate system the terms in the expression (10) assume the form

$$W_Z=-H_0M_0[\cos(\varphi_H-\varphi_1)+\cos(\varphi_H-\varphi_2)],$$
$$W_E=A_EM_0^2\cos(\varphi_1-\varphi_2),$$
$$W_D=-A_DM_0^2\sin(\varphi_1-\varphi_2),$$

where f is given by the expression (9). These quantities are, respectively, the Zeeman interaction, the intersublattice exchange interaction, and the Dzyaloshinskiĭ interaction. Here M_0 is the saturation magnetization of the sublattice; φ_1 and φ_2 are the azimuthal angles of the sublattices; φ_H is the angle of the magnetic field, measured from the C_2 axis; A_E and A_D are corresponding constants.

In the expression (10) the term describing the anisotropy in the basal plane has been dropped. The contribution arising from the impurity subsystem will be obtained below.

The equilibrium angles of the magnetizations of the sublattices are determined from the condition of an energy minimum

$$\partial W/\partial\varphi_k=0 \quad (k=1,2) \tag{11}$$

where $\varphi_1-\varphi_2=\pi-\delta_1-\delta_2$ and δ_k are the cant angles of the sublattices. If the sublattices are identical and the impurities are distributed with equal probability over the sites of the sublattices, then $\delta_1=\delta_2=\delta$.

From Eq. (11) we obtain the cant angle for $\delta\ll 1$:

$$\delta\approx(H_0M_0+A_DM_0^2-\partial f/\partial\varphi_1)/2A_EM_0^2. \tag{12}$$

where it was assumed that under the condition of equilibrium $\varphi_1=\varphi_H-\delta+\pi/2$.

In the experiment we measured the change in the magnetic moment, whose magnitude, as is well known,[17] is determined by the expression

$$|\mathbf{m}|=|\mathbf{M}_1+\mathbf{M}_2|=2M_0\sin\delta\approx 2M_0\delta. \tag{13}$$

If the optical irradiation introduces a change via redistribution of the populations of the levels of the impurity centers, then the contribution of the magnetization of the first sublattice to the change photoinduced in the moment is

$$\delta m_{l1}\approx[\partial(\Delta f)/\partial\varphi_1]/2A_EM_0, \tag{14}$$

where $\Delta f=f^*-f^0$, f^0 corresponds to the populations of the levels of the center in the absence of radiation, i.e., when $A_1=A_2=0$, and f^* corresponds to the populations when A_1 and A_2 are nonzero. Since the sublattices make the same contribution to the energy f and the centers located at the corresponding positions of different sublattices have the same energies, we have

$$\delta m_l=2\delta m_{l1}. \tag{14'}$$

In calculating the photoinduced changes of the magnetic state, in order to compare with experiment it is necessary to take into account the fact that the sample is in an unsaturated state and its magnetization is a function of the magnetic field. As customarily done in the literature,[17,18] we change in the expression for f from the variables $\mathbf{M}_1$ and $\mathbf{M}_2$ to the variables $\mathbf{m}$ and $\mathbf{L}$. This gives

$$\mathbf{M}_1=(\mathbf{m}+\mathbf{L})/2, \quad \mathbf{M}_2=(\mathbf{m}-\mathbf{L})/2$$

under the condition that $\mathbf{mL}=0$. Here the magnetization of the crystal depends on the magnetic field $m=m(H_0)$. In the model calculations below we employ the very simple dependence

$$|m(H_0)|=a\,\mathrm{arctg}[(H_0-b)/b]+C, \qquad (15)$$

obtained in the quadratic (in the field) approximation of the inverse susceptibility.[19]

The calculations were performed for the parameter values $D=3.865\cdot10^{-14}$ ergs, $E=3.796\cdot10^{-14}$ ergs, $a=33$, $b=150$, and $C=26$. It was also assumed that the exchange field acting on an impurity ion is equal in magnitude to the field acting on the Fe^{3+} ion in $FeBO_3$. This gives $\lambda L\beta\tilde{S}=0.208\cdot10^{-15}\cdot F(T)$ ergs and, $\lambda m\beta\tilde{S}=0.338\cdot10^{-17}\cdot F(T)\cdot m(H)$ ergs, where $F(T)$ is a polynomial of degree 10 for fitting the temperature dependence of the magnetization of $FeBO_3$. All other parameters are identical to the parameters given in the literature. The best fit to the experimental data with this collection of parameters was obtained with $\alpha=22.5°$ and an impurity concentration $N_0=10^{16}$.

RESULTS AND DISCUSSION

Since optical irradiation populates predominantly the state $|2\rangle$, in order to understand the effect on the magnetic system of the crystal, we set for simplicity $d^{2\psi}=d^{\psi 1}=0$ and, because the lifetime of the center in the optically excited state is short, $n^{\psi}=0$. We assume that the probabilities of optical transitions are the same for all positions. In this case $A_1=0$ and the constant A_2 was calculated from the condition that the deviation of the population of the state $|2\rangle$ from equilibrium for centers in positions $t=3$ and 6 as a result of optical irradiation at $T=4.2$ K was 5, 10, 20, 30, and 50%, corresponding to the values $A_2=0.068$, 0.142, 0.318, 0.545, and 1.271. To determine the range of values of the probability of the optical transition $d^{1\psi}$ we employed the fact that at liquid-helium temperatures the ratio of the "weak-field dip" in the $\delta m_l(H)$ dependence in Fig. 3 to the magnitude of the second dip is about 1/4.

Figures 7 and 8 show the computation results for the case when the field H_0 is perpendicular to the C_2 axis for different levels of optical pumping and different temperatures, respectively. As in the experiment, we obtained two dips in the field dependence of δm_l, and the asymptotic level was reached in strong magnetic fields. These dips are due to the competition between the contributions from centers located in the positions $t=2$, 5 (low-field dip) and $t=3$, 6 (high-field dip) (see inset in Fig. 7). The centers located in positions of the type $t=1$, 4 are not manifested because of the large splitting between the energy levels and the practically zero population of the state $|1\rangle$.

According to Fig. 7, as the optical radiation power increases the centers located at the positions $t=2$, 5 react more strongly to the radiation. This behavior is explained by the fact that the splitting of the energy levels for centers in positions of the type $t=2$, 5 is somewhat larger than in the positions $t=3$, 6. At a fixed temperature the thermodynamically equilibrium population of the state $|1\rangle$ for centers

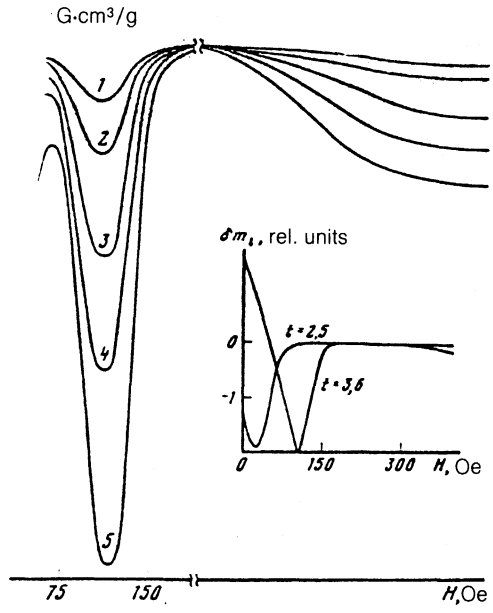

FIG. 7. Field dependences of the photoinduced change in the magnetic moment (calculation) at $T=4.2$ K and $A_2=0.068$ (*1*), 0.142 (*2*), 0.318 (*3*), 0.545 (*4*), and 1.271 (*5*). Inset: contributions from centers occupying different crystallographic positions.

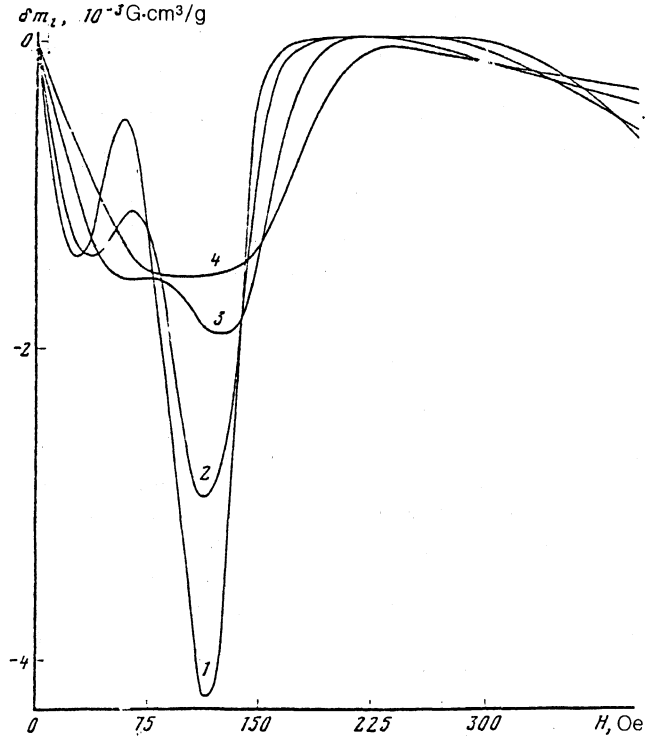

FIG. 8. Field dependences of the photoinduced change in the magnetic moment at different temperatures (calculation) with $A_2=0.318$ and $T=4.2$ K (*1*), 6 K (*2*), 10 K (*3*), and 16 K (*4*).

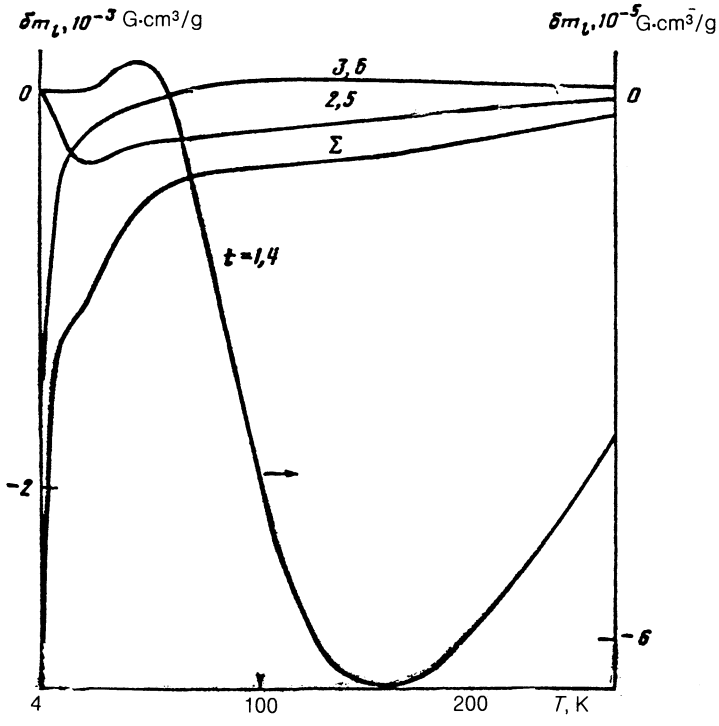

FIG. 9. Temperature dependences of the photoinduced change in the magnetic moment (calculation) with $A_2 = 0.318$, $H = 100$ Oe: contributions from centers in different crystallographic positions, Σ—integral curve $H = 100$ Oe.

$t = 2, 5$ is higher than the population of the analogous state for centers $t = 3, 6$, and since the populations of levels with ε_{pq}^2 increases with increasing optical radiation power, the fraction of centers transferred from the state $|1\rangle$ into the state $|2\rangle$ will be larger for $t = 2, 5$ centers. It is obvious that in the high-power limit these fractions will become equal and both dips will become identical. This tendency is observed in both the experiment and in the calculations (compare Figs. 4 and 7).

The change in the photoinduced moment at fixed optical pump power and different temperatures can be explained on the basis of the above considerations (Fig. 8). In this case we find that the depth of one of the dips changes insignificantly while the depth of the other changes much more strongly. For $T > 16$ K both dips merge and subsequently behave as a single entity. It is obvious that at high temperatures the populations of the states $|1\rangle$ for different centers become equal, and the fractions of the centers participating in phototransitions become equal.

The temperature dependence of the photoinduced change in the magnetic moment, calculated in a magnetic field $H = 100$ Oe, is shown in Fig. 9 (central curve–Σ). Curves of the temperature dependences of the contributions from centers in different crystallographic positions are also presented there. We call attention to the good agreement at low temperatures between experiment (Fig. 5) and the calculations (Fig. 9). As the optical radiation power increases, the photoinduced component of the magnetic moment increases in magnitude, and the role of the centers with large energy splittings and their relative contributions increase with decreasing temperature. Experimentally, the situation is significantly more complicated, since it must be recognized that the thermomagnetic contribution to the matrix become noticeable and the domain structure and its dynamics are changed with increasing temperature. In the case of high temperatures ($T > 50$ K) secondary effects (heating, elastic stresses) can mask the mechanism being considered for the photomagnetic effect in $FeBO_3$ crystals, and all mechanisms must be taken into account simultaneously.

The theoretical results make it possible to understand why irradiation produces in the crystal an effective field which is perpendicular to the direction of the external magnetic field and is recorded through the change in the linear birefringence.[4] Since these experiments were performed at temperatures $T \geqslant 78$ K, the states $|1\rangle$ and $|2\rangle$ for centers analogous to centers in the positions $t = 2, 5$ $(-\alpha)$ and $t = 3, 6$ $(+\alpha)$ and having small splittings are equally populated, and because the thermal relaxation is fast ($\Delta/k_B T \ll 1$), the optical radiation hardly disrupts their thermodynamically equilibrium populations. For centers in positions of the type $t = 1, 4$ the splitting is much stronger, and the population of the state $|1\rangle$ and correspondingly the contribution to the photoinduced redistribution of the level populations increase with the temperature. As follows from the expression (4), the interaction of the impurity spin with the magnetization vector of the sublattice, which is perpendicular to the external magnetic field, is stronger. For this reason, for centers of the type $t = 1, 4$ it is the component of the field along the sublattice magnetization that increases when the state $|1\rangle$ is emptied.

We can say the following concerning the self-excited oscillations (in time), observed at low temperatures, in the photoinduced part of the magnetic moment. This effect was first reported in Ref. 20, where oscillations of the magnetic permeability were observed in $Y_3Fe_5O_{12}$:Si^{4+} crystals under irradiation. The results were interpreted as oscillations of the domain structure. The results of experiments on the visualization of the photoinduced motion of domain walls in a gradient magnetic field were presented later in Ref. 21. It was found that the instability of the domain structure is caused by competition between the anisotropy from two types of centers, which react differently to irradiation.

Photoinduced motion of domain walls has also been observed in $FeBO_3$ crystals,[5] and the parameters characteriz-

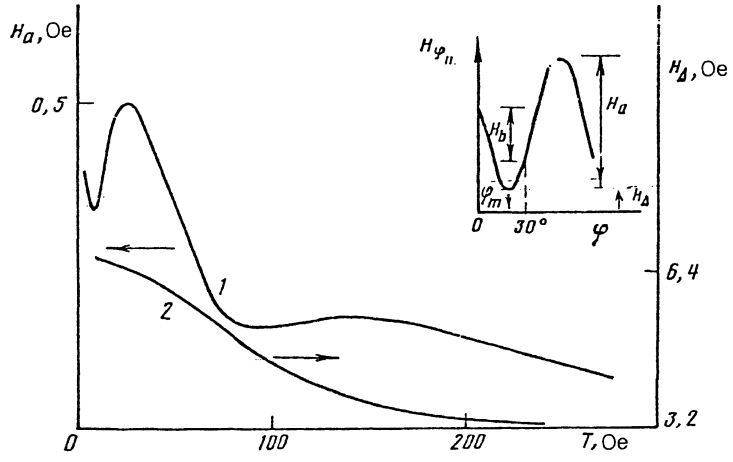

FIG. 10. Temperature dependences (calculation) of the anisotropic part of the field of the impurity subsystem (*1*) and the isotropic contribution (*2*). Inset: angular dependence of the field generated by the impurity centers.

ing the domain structure were investigated as a function of the magnetic field strength and the optical radiation power. Several mechanisms were proposed to explain this effect: photoinduced phase transition, caused by softening of the magnetoelastic mode;[22] self-excited oscillations of the parametric type;[23] instability due to competition between different anisotropies.[24]

In our case, self-excited oscillations are observed in a limited range of magnetic fields and at temperatures below 6 K. This suggests that the instability of the optically excited magnetic system of $FeBO_3$ could be associated with competition between magnetic anisotropies and restructuring of the magnetic state of the crystal. However, currently available experimental data are insufficient to suggest a definite model for the process.

SPIN-REORIENTATIONAL TRANSITION IN THE BASAL PLANE

The correctness of the model employed for the impurity center is further confirmed by the description of, in addition to the photomagnetic properties, the anisotropic properties of $FeBO_3$ and the fact that a spin-reorientational transition occurs at low temperatures.

We consider only the contribution of the impurity subsystem. Since all terms in Eq. (10), except for f, are isotropic with respect to rotation of the magnetization vector in the basal plane, it is the anisotropy f that could be responsible for the properties of interest to us. The internal field, generated by the impurity subsystem and acting on the magnetic moment of the crystal, is determined by the expression[18]

$$H_{\varphi_m} = -(\partial f/\partial \varphi_m)/M_0, \qquad (16)$$

where φ_m is the angle between the magnetic moment of the crystal and the chosen axis of the crystal (in our case the C_2 axis), and M_0 is the magnetization of the sublattice.

Calculation of the field (16) in the absence of optical radiation, i.e., for $A_1 = A_2 = 0$, gives a dependence of the type shown in the inset in Fig. 10. It is seen that an alternating part H_a is observed against the background of a constant component H_Δ. As the temperature changes, the angular position of the minimum of H_a changes. If the temperature increases, the amplitude of the variable part passes through a maximum and then approaches zero. The constant component also approaches zero as the temperature increases (see Fig. 10).

It is obvious that the energy of the magnetic system will be a minimum at the positions φ_m^0. It is these directions that will be the directions of easy magnetization. The temperature dependence of φ_m^0 is shown in the inset in Fig. 11. One can see that the easy-magnetization axis turns from $\varphi_m^0 = 30°$ to the angle $\varphi_m^0 = 0$ in the temperature range 4–30 K. If curves of the type presented in the inset in Fig. 10 are analyzed, as done in Ref. 25, i.e., the anisotropy field is defined as the difference of the resonance fields corresponding to the angles $\varphi_H = 30°$ and $\varphi_H = 0°$,

$$\delta H_p = H_p(\varphi_m^0 = 30°) - H_p(\varphi_m^0 = 0) \sim H_b,$$

then we obtain the curve presented in Fig. 11 (curve *1*). Curve *2* in the same figure was calculated with the exchange interaction of the impurity spin with the matrix two times smaller than for curve *1*. In all calculations the impurity concentration was $N_0 = 10^{16}$ cm^3. These curves are qualitatively similar to curve *3*, taken from Ref. 25 and determined as the anisotropy field in the basal plane. Using the terminology adopted in magnetoresonance studies, the constant part H_Δ in Fig. 10 behaves as a function of the temperature like an "isotropic gap" Δ, and the amplitude of the alternating part H_a behaves similarly to the AFMR linewidth. For nonuniformly magnetized media with strong local anisotropy, this behavior of the linewidth is expected, and in this case the damping of the microwave oscillations, which is determined by the imaginary part of the frequency ω'', is proportional to $(H_E H_a)^{1/2}\theta$, where the factor θ does not exceed unity.[18] The existence of "partial minima" of the anisotropy field at low temperatures $T < T_S$ could be the reason for the irreversible behavior of the resonance parameters with increasing or decreasing temperature as well as splitting of the AFMR line.

We did not employ in our calculations the optimal energy parameters of an impurity center in the $FeBO_3$ matrix, and the values of the parameters are probably too high. At the present time, however, there are no published data on these quantities. Nevertheless, we obtain quite good agreement between theory and experiment for the photomagnetic effect. In calculating the spin-reorientational transition in the basal plane, we fall into the range of values of anisotropy fields determined experimentally by other methods,

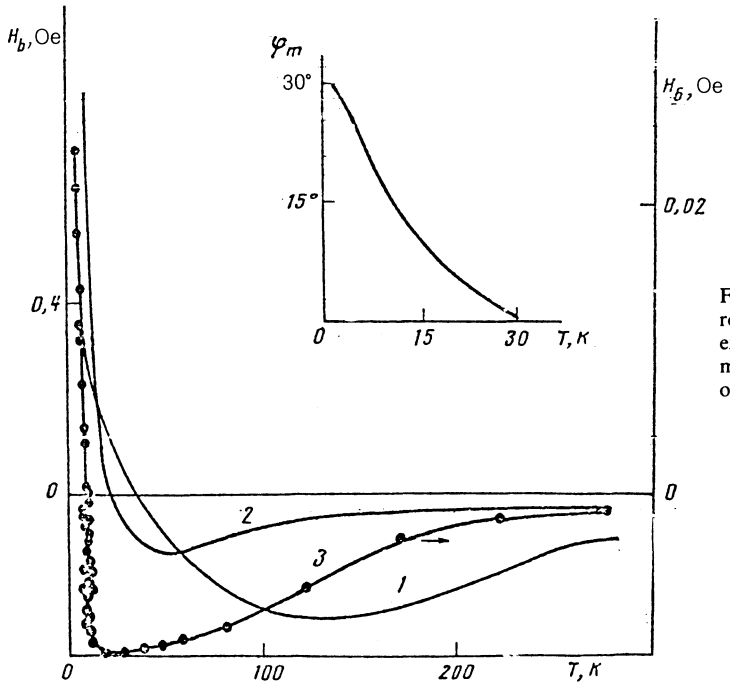

FIG. 11. Temperature dependences of the field of the magnetic anisotropy in the basal plane (see text): *1,2*—calculation (for curve *2* the exchange interaction is two times smaller than for curve *1*), *3*—experiment (H_6 (Ref. 25)). Inset: temperature dependence of the direction of easy magnetization in the basal plane.

$H_a \approx 0.01$–0.7 Oe. We note that the magnitude of this anisotropy and the value of T_S depend on the quality of the sample.[7] These quantities are higher for samples of lower quality. This is seemingly attributable to the fact that as the number of defects, i.e., Fe^{2+} ions, having strong spin-orbital coupling increases, stresses in the crystal intensify and this in turn increases the crystal-field parameters D and E and alters the exchange between an impurity spin and the matrix.

CONCLUSIONS

It follows from the foregoing analysis of the experimental and theoretical data that the photomagnetic and anisotropic properties of $FeBO_3$ crystals can be described within a model where the impurity center (tentatively an Fe^{2+} ion) is a three-level center whose lower energy levels cross, and the crystal matrix is described in the continuous approximation. Optical irradiation induces, together with charge transfer between heterovalent iron ions,[7,8] redistribution of the populations of the sublevels of the ground state multiplet of the impurity center, and the level with strong anisotropic behavior is predominantly populated. The calculations show that the observed photoinduced change of magnetization in weak magnetic fields is determined by the state of the macroscopic magnetization of the crystal. The splitting of the energy levels, which is associated with the exchange interaction of an impurity spin with the antiferromagnetism vector, is the main effect and determines the temperature dependence of the photoinduced changes and anisotropic properties of the crystal. The anistropic properties, including the spin-reorientational transition, are explained by the competition between the fields which arise from centers located in nonequivalent crystallographic positons with respect to the direction of the magnetic moment.

The approach employed in this paper explains qualitatively the main features of the experimental curves. More complete agreement between the calculations and the experiments can be obtained by determining more accurately the energy spectrum of an impurity center, taking into account the anisotropy of the exchange interactions of an impurity spin with both sublattices of the crystal. In addition, the temperature and angular dependences of the optical transition probabilities must be studied further and the dynamics of the electronic transitions between levels of the ground state multiplet must be considered in greater detail. To explain the self-excited temporal oscillations of the magnetization, additional experimental investigations must be performed and a mathematical model must be specified.

In conclusion we thank V. V. Rudenko and N. V. Volkov for fruitful discussions and helpful suggestions.

[1]N. V. Volkov and G. S. Patrin, Prib. Tekh. Eksp. **5**, 118 (1990).
[2]D. E. Lacklison, J. Chadwick, and J. L. Page, J. Appl. Phys. **42**, 1445 (1971); J. Phys. D **5**, 810 (1972).
[3]M. H. Seavy, Solid State Commun. **12**, 49 (1973).
[4]Yu. M. Fedorov, A. A. Leksikov, and A. E. Aksenov, Zh. Eksp. Teor. Fiz. **89**, 2099 (1985) [Sov. Phys. JETP **62**(6), 1211 (1985)].
[5]Yu. M. Fedorov, A. A. Leksikov, and O. V. Vorotynova, Solid State Commun. **55**, 987 (1985); J. Magn. Magn. Mater. **68**, 383 (1987).
[6]G. A. Petrakovskii, G. S. Patrin, and N. V. Volkov, Phys. Status Solidi A **87**, K153 (1985).
[7]G. S. Patrin, G. A. Petrakovskii, and V. V. Rudenko, Phys. Status Solidi A **99**, 619 (1987).
[8]G. A. Petrakovskii and G. S. Patrin, in *Abstracts of Reports at the 24th All-Union Conference on Low-Temperature Physics* [in Russian], Tbilisi, 1986, Part 3, p. 105.
[9]D. A. Velikanov, G. S. Patrin, G. A. Petrakovskiĭ, and V. E. Volkov, Preprint No. 586F, Institute of Physics of the Siberian Branch of the USSR Academy of Sciences, Krasnoyarsk, 1989.
[10]C. A. Bates and P. Steggles, J. Phys. C **8**, 2283 (1975).
[11]K. W. H. Stevens and D. Walsh, J. Phys. C **1**, 1554 (1968).
[12]R. Wolfe, A. J. Kurtzig, and R. C. le Craw, J. Appl. Phys. **41**, 1218 (1970).
[13]H. Pollak, R. Quartier, W. Bruyneel, and P. Walter, J. de Phys. **37**, Suppl. No. 12, C6-589 (1976).
[14]K. J. Rao, Proc. Indian Nat. Sci. Acad. A **52**, 176 (1986).
[15]E. Stryjewski and N. Giardano, Adv. Phys. **26**, 487 (1977).
[16]G. A. Petrakovskii and G. S. Patrin, Zh. Eksp. Teor. Fiz. **90**, 1769 (1986) [Sov. Phys. JETP **63**(5), 1038 (1986)].
[17]E. A. Turov, *Physical Properties of Magnetically Ordered Crystals* [in Russian], Nauka, Moscow, 1963.

[18]A. G. Gurevich, *Magnetic Resonance in Ferrites and Antiferromagnets* [in Russian], Nauka, Moscow, 1973.
[19]R. Bozorth, Ferromagnetism, Van Nostrand, N.Y., 1951.
[20]V. F. Kovalenko, I. I. Kondilenko, and P. S. Kup, Zh. Eksp. Teor. Fiz. **74**, 734 (1978) [Sov. Phys. JETP **47**(2), 386 (1978)].
[21]V. G. Veselago, I. V. Valdimirov, R. A. Doroshenko, and M. S. Setchenkov, Fiz. Tverd. Tela **29**, 2758 (1987) [Sov. Phys. Solid State **29**, 1585 (1987)].
[22]Yu. M. Fedorov, A. F. Sadreev, and A. A. Laksikov, Zh. Eksp. Teor. Fiz. **93**, 2247 (1987) [Sov. Phys. JETP **66**(6), 1283 (1987)].
[23]B. A. Iranov and S. N. Lyakhimets, Pis'ma Zh. Eksp. Teor. Fiz. **46**, 23 (1987) [JETP Lett. **46**, 26 (1987)].
[24]A. K. Zvezdin and A. A. Mukhin, Pis'ma Zh. Eksp. Teor. Fiz. **42**, 129 (1985) [JETP Lett. **42**, 157 (1985)]; Kratkie soobsheniya po fizike FIAN, No 5, 20 (1988).
[25]V. D. Doreshev, I. M. Krygin, S. N. Lukin *et al.*, Pis'ma Zh. Eksp. Teor. Fiz. **29**, 286 (1979) [JETP Lett. **29**, 257 (1979)].

Translated by M. E. Alferieff